MULTIPHASE FLOW EXPERIMENTS AND INSTRUMENTATION

1. Flow Structure of Nonequilibrium Dispersed Flow Through Heated Bends, *M. J. Wang, F. Mayinger (Tech Univ of Munich-Germany)*

Nonequilibrium dispersed two-phase flow can be encountered in nuclear reactor systems under normal and accidental conditions. Previous studies on this topic are mostly limited to simple pipe flows. Dispersed flow in complex geometries like bends and coils, which are being used in practice, is, however, still poorly understood. To that end, this study concentrates on the flow structure of the nonequilibrium dispersed two-phase flow through heated 90-deg circular bends based on experiment and theoretical analysis.

In evaluating the nature of the high-quality dispersed flow, the behavior of the bulk vapor flow is of fundamental importance. Such three-dimensional developing flow is analyzed through single-phase computation as a first approximation. It is revealed that even for large bend-to-tube radius ratios of 28 and 42, there is an appreciable fluid acceleration at the outer side and deceleration at the inner side of the bend. More important is that a double-vortex secondary flow develops early in the bend and reaches a maximum at the middle of the bend, which accounts for ~8 to 10% of the mean velocity. It is further indicated from computation that the single-phase flow structure depends mainly on the curvature ratio when the Reynolds number changes within a factor of 10 in the turbulent region.

Based on the quantitative single-phase flow field, the dynamics of liquid droplets entrained in the superheated vapor stream is evaluated by a Lagrangian model coupling the force and energy balance. The effect of the turbulence is simulated through a stochastic treatment considering the interactions between the droplets and energy containing turbulent eddies. Analytical results provide some intrinsic aspects of the mechanism of dispersed flow structure. Liquid droplets with small dimension are subjected to strong actions of the turbulent dispersion, the secondary flow, and the thermal evaporation. In the high nonequilibrium flow, they tend to fully evaporate soon after entering the bend. However, in the slightly nonequilibrium region, a random nature of droplet trajectories is found, which results in a wide range of droplet deposition on the bend wall. When droplets are $>100\ \mu m$, they tend to be less influenced by the aforementioned factors. Particle inertia in this case plays a key role in most of the region. The secondary flow may be important only in the limited region very close to the wall, which drives the droplets moving toward the inner side. For even larger droplets over $250\ \mu m$, the inertial effect dominates the process of droplet motion, keeping droplets moving toward the outer side of the symmetric plan. Note, however, that the thermal repelling force initiated by the nonuniform evaporation is not sufficiently large to resist the inertial action. Droplets appear to be able to contact directly on the hot wall, even over the Leidenfrost temperature.

The nature of the nonequilibrium dispersed-flow structure is extensively investigated in a refrigerant R-12 two-phase loop. Systematic measurements were performed for a wide range of mass flow rate from 400 to 2000 $kg/m^2 \cdot s$, wall heat flux from 20 to 60 kW/m^2, bend-to-tube radius ratio from 28 to 42, and reduced pressure 0.23 under postdryout conditions. A method of local liquid fraction measurement by an impedance probe has been used to determine the liquid distribution in the cross section and in the axial direction.

A significant departure of the dispersed-flow structure from that in straight channels is confirmed from measurements. The inertial effect of two phases with different densities produces a remarkable process of phase separation that takes place at the entrance and develops quickly at the beginning of the bend. More than half the liquid droplets are found to accumulate soon in the outer side region within the first 15 deg of the bend angle. Further increase in liquid concentration in that region continues to 45 deg. Measurements indicate that under large mass flow rates, a high deposition flux of liquid droplets tends to induce rewetting on the outer wall. From the middle of the bend, the behavior of flow structure depends critically on the combined effect of secondary flow transportation and wall heat transfer. Under nonrewetting, phase separation dominates, and only a small number of droplets can be driven to the inner side. However, for rewetting status, a redistribution process develops by which a large amount of liquid in the form of film is found to be stretched from the outer to the inner side.

Parametrically, the dispersed-flow structure is greatly influenced by the mass flow rate that corresponds to the specific bulk velocity and initial droplet size. The measurements also indicate that wall heat flux does not seem to be important except when it induces a change of heat transfer pattern. Another major parameter in the dispersed flow structure is the ratio of the bend to tube radius that changes the magnitude of the centrifugal force and the secondary flow.

This study of the structure of nonequilibrium dispersed flow provides a sound basis for the analysis of dispersed-flow heat transfer in curved channels.

2. Direct Containment Heating Experiment for Annular Reactor Cavity Geometry, *Martin Lopez de Bertodano (Purdue Univ)*

INTRODUCTION

The high-pressure ejection of molten core material from the vessel of a nuclear reactor would cause dispersal and small droplet formation, which leads to direct containment heating (DCH). As a consequence, the pressure in the containment would rise. Also, the chemical reactions between the corium droplets and the steam would produce hydrogen, adding another source of pressurization.

The objective of this work is to perform a separate-effects experiment to obtain data for corium dispersal and droplet size distribution for an annular reactor cavity geometry. These data could then be used to develop correlations for the source terms in a computer code for containment pressure evaluation.

To formulate models for mass dispersal and droplet size distribution, it is essential to understand the droplet entrainment mechanisms. Once this is known, the heat transfer and chemical reaction rates may be calculated to determine the level of pressurization. However, the mechanisms of droplet entrainment are complicated and the conditions are different from the well-known cases (i.e., annular flow), so experimental work is required. A good review of DCH experiments has been provided by Corradini.[1] These experiments have simulated the Zion cavity and containment configuration, and the focus has been on measuring the containment pressure. There are practically no separate-effects data, such as droplet size dis-

tribution. Therefore, it is difficult to develop mechanistic models. Moreover, droplet entrainment and mass dispersal are strongly dependent on containment geometry. Therefore, experiments are needed for different geometries to Zion.

DESCRIPTION OF THE ACTUAL WORK

A series of high-pressure melt ejection (HPME) tests have been conducted on a $\frac{1}{20}$ linear scale model of a nuclear reactor annular cavity. The tests were carried out at pressures up to 6.8 MPa (1000 psi) and room temperature. The molten fuel has been simulated with woods-metal and water, the steam with nitrogen and helium.

The experiment was scaled according to droplet entrainment in the cavity. It was assumed that the corium forms a film along the outward wall of the cavity and is entrained by the high-velocity steam. Hence the flow of liquid and gas in the cavity annulus, which is long and narrow, was assumed to be similar to annular flow in pipes. The scaling criterion is the ratio of the time constant for entrainment to the residence time of a liquid film particle in the cavity:

$$\theta = \frac{\tau_\varepsilon}{\tau_{lf}} = \frac{Re_f}{En} \frac{1}{L_c/D_h} ,$$

where *En* is the entrainment number given by Kataoka and Ishii's[2] correlation for droplet entrainment in annular flow.

The other important quantity in HPME is the droplet size. For scaling purposes, Kataoka and Ishii's droplet size correlation[3] for annular flow was used.

The preliminary calculations using a one-dimensional isentropic compressible flow model indicate that there is choking in the cavity because the area ratio of orifice size to annulus size is large enough.

One test was performed with helium and water. The scaling calculations indicate that the level of entrainment for this test is similar to the prototypical case.

Six tests were done with gas and woods-metal. Woods-metal is a heavy alloy that has a very low melting point. Its transport properties and some physical properties such as density are very close to that for corium. Because of scaling constraints, the level of woods-metal entrainment expected is low compared to the prototypical case (i.e., the values of θ are higher, so most of the liquid leaves the cavity before being entrained). On the other hand, the droplet size predicted for woods-metal is greater than for water and gets closer to the prototypical droplets.

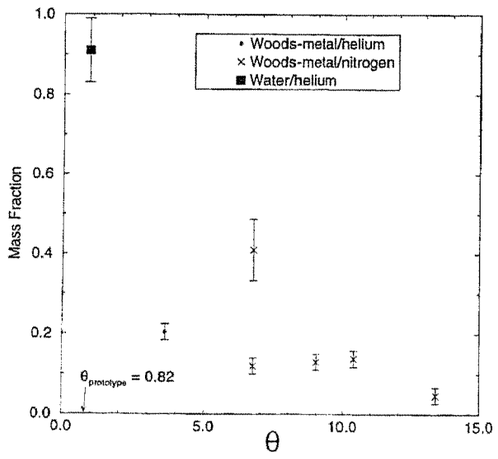

Fig. 1. Entrained mass compared with scaling criterion.

RESULTS

High levels of entrainment were observed in the helium-water experiment because of choking in the narrow annular cavity (see Fig. 1). The entrained mass fraction was 91%. For the most severe woods-metal tests, 2 kg were entrained out of a maximum possible 15 kg. The level of entrainment for these tests is considerably lower than for the prototypical case because of scaling limitations.

In comparisons between the data and the correlation of Kataoka and Ishii,[3] the size of the entrained droplets was four times larger than the prediction for woods-metal and three times larger for water. Extrapolating this result, the size of the entrained droplets for the prototypical case would be ~1 mm. Although the validity of this extrapolation is not certain, there is no way to make a better estimate at the present time.

The maximum pressure in the cavity was between 0.5 and 0.6 MPa (70 and 90 psia), so the integrity of the main components is not threatened. However, these pressures indicate choking and high entrainment.

1. M. CORRADINI, "Direct Containment Heating," *Fission Product Transport Processes in Reactor Accidents*, J. T. ROGERS, Ed., Hemisphere Publishing, New York (1990).

2. I. KATAOKA, M. ISHII, "Mechanism and Correlation of Droplet Entrainment and Deposition in Annular Two-Phase Flow," NUREG/CR-2885, ANL-82-44, Argonne National Lab. (1982).

3. I. KATAOKA, M. ISHII, K. MISHIMA, "Generation and Size Distribution of Droplet in Annular Two-Phase Flow," *Trans. ASME*, **105**, 230 (1983).

3. Reflux Cooling Experiments on the NCSU Scaled PWR Facility, *J. Michael Doster, Eric Giavedoni (NCSU)*

INTRODUCTION

Under loss of forced circulation, coupled with the loss or reduction in primary side coolant inventory, horizontal stratified flows can develop in the hot and cold legs of pressurized water reactors (PWRs). Vapor produced in the reactor vessel is transported through the hot leg to the steam generator tubes where it condenses and flows back to the reactor vessel. Within the steam generator tubes, the flow regimes may range from countercurrent annular flow to single-phase convection. As a result, a number of heat transfer mechanisms are possible, depending on the loop configuration, total heat transfer rate, and the steam flow rate within the tubes. These include (but are not limited to) two-phase natural circulation, where the condensate flows concurrent to the vapor stream and is transported to the cold leg so that the entire reactor coolant loop is active, and reflux cooling, where the condensate flows back down the interior of the coolant tubes countercurrent to the vapor stream and is returned to the reactor vessel through the hot leg. While operating in the reflux cooling mode, the cold leg can effectively be inactive. Heat transfer can be further influenced by noncondensables in the vapor stream, which accumulate within the upper regions of the steam generator tube bundle. In addition to reducing the steam generator's effective heat transfer area, under these conditions operation under natural circulation may not be possible, and reflux cooling may be the only viable heat transfer mechanism. The scaled PWR (SPWR) facility in the nuclear engineering department at North Carolina State University (NCSU) is being used to study the effectiveness of two-phase natural circulation and reflux cooling under conditions associated with loss of forced circulation, midloop coolant levels, and noncondensables in the primary coolant system.

FACILITY DESCRIPTION

The NCSU SPWR facility is a Freon-based one-ninth scale model of a two-loop Westinghouse PWR. The reactor core is simulated by electrically heated rods with heater power governed by either a point reactor kinetics model or set manually at an operator-designated power level. The reactor kinetics model is coupled through the system's instrumentation so that reactivity feedback effects (Doppler, moderator temperature, etc.) control the reactor's dynamic response. Both primary and secondary sides are represented, including such normal balance-of-plant components as condensers, condensate and feed pumps, and feedwater heaters. A photograph of the facility is provided as Fig. 1.

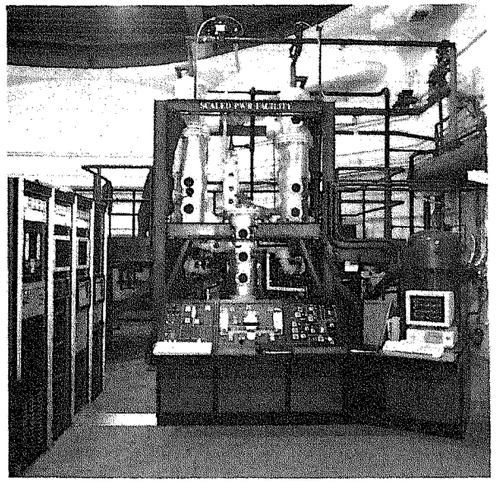

Fig. 1. The NCSU SPWR facility.

REFLUX COOLING EXPERIMENTS

A series of reflux cooling experiments have been run on the SPWR facility to measure steady-state heat transfer rates as a function of primary- and secondary-side pressure. The SPWR facility is a two-loop facility, with the individual coolant loops designated as the A and B sides. The B-side steam generator was isolated in each of these runs. Steam generator level was maintained so that the tube bundle region was completely flooded, and the steam generator operated in its normal recirculation mode. The primary side of the SPWR facility was drained to midloop coolant levels from nominal operating temperatures and pressures and stabilized prior to initiation of significant secondary-side steaming. Countercurrent, horizontal stratified flow in the hot leg and stagnant conditions in the crossover leg were verified visually through the glass viewing windows located in these areas.

The reactor kinetics model receives reactivity inputs from three sources: (a) simulated control rod motion, (b) moderator temperature, and (c) core power. The SPWR facility will "load follow" in a manner similar to an actual power plant, based on the average loop temperature as measured by the hot- and cold-leg resistance temperature detectors. For steady-state studies, the reactor power is controlled indirectly through the steaming rate and the corresponding steam generator pressure by manually opening and closing the main steam throttle valve. The kinetics model includes a preprogrammed rod worth

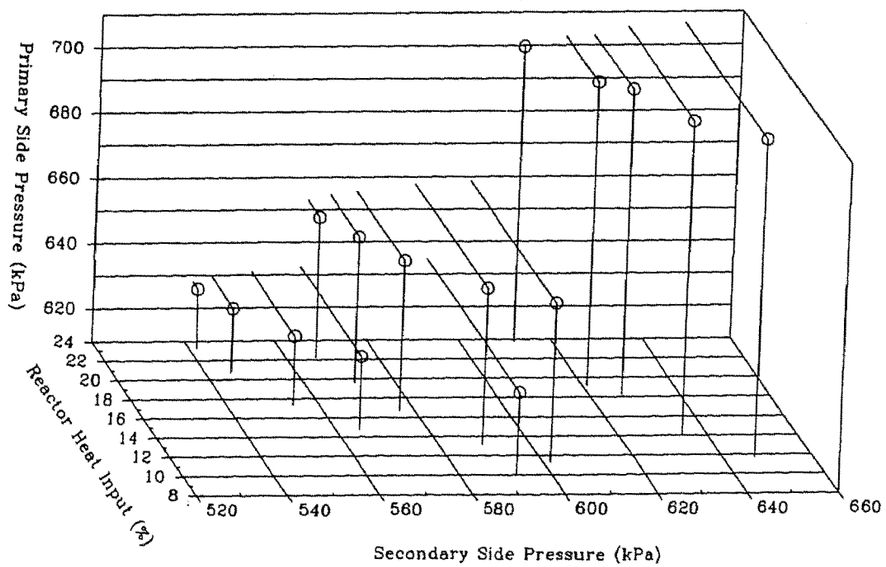

Fig. 2. Primary-side pressure compared with heat transfer rate and secondary-side pressure at constant steam generator level.

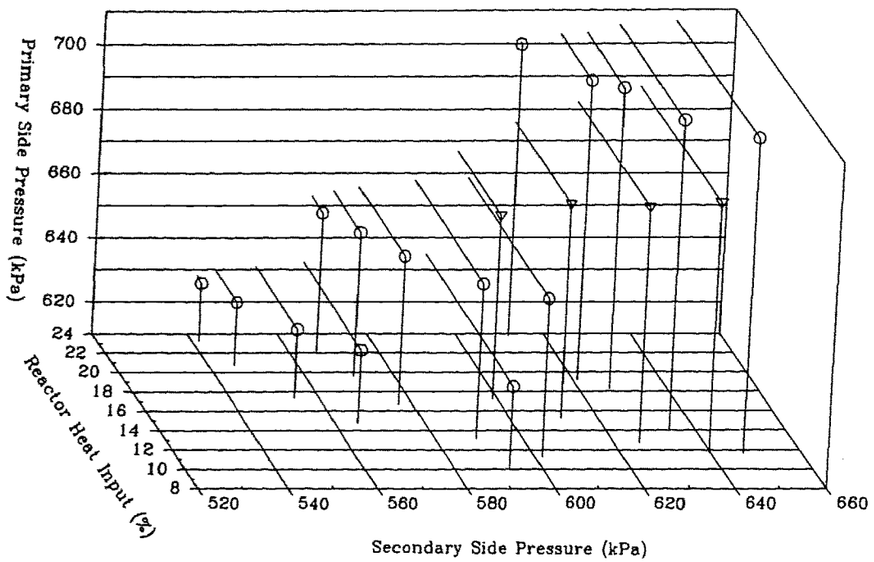

Fig. 3. Comparison of heat transfer results with and without feed flow.

curve, which gives reactivity as a function of rod position. Primary-side pressure and temperature are determined by control rod position.

Steaming rates were changed in steps to produce approximately equal changes in secondary-side pressure. For these runs, control rod position was held constant after each insertion, resulting in slight variations in primary-side pressure as the steaming rate was varied. Minor adjustments in rod position at each power level can be used to reduce these variations if desired. Steady-state values are plotted in Fig. 2 as primary-side pressure compared with reactor power and steam generator pressure. The reactor power is given as the percent of nominal full power (80 kW). The clear functional relationship between these variables is apparent.

A separate experiment was run at relatively low steaming rates in the absence of feed flow. Steam generator level was allowed to decrease continuously, while reactor power and primary- and secondary-side pressures went to steady state. The steam generator was then refilled prior to changing the steaming rate. At no point did the steam generator level approach the minimum level necessary for recirculation to occur. These data are shown in Fig. 3 as the triangular data points superimposed on the results of the previous experiment. Variability in the primary-side pressure is much more evident in these results, illustrating the importance of feed flow rate and feed temperature on the heat transfer rate.

4. Preliminary Tests Using Magnetic Resonance Imaging of Two-Phase Flow Patterns and Transitions, *Jose N. Reyes, Jr. (Oregon State Univ), David Saloner (Univ of California, San Francisco), Abd Y. Lafi (Oregon State Univ)*

INTRODUCTION

This paper presents the results of preliminary tests used to establish the feasibility of using magnetic resonance imaging (MRI) to examine and quantitatively characterize two-phase flow patterns and flow transitions. These tests were performed at the University of California, San Francisco (UCSF) School of Medicine MRI Center as a collaborative research effort with Oregon State University (OSU). Special scanning sequences designed by UCSF for flow imaging were implemented in the tests. UCSF operated the MRI facility, and OSU constructed and operated a cocurrent air-water flow loop (Fig. 1) consisting of a 1-in.-diam test section capable of producing air superficial velocities j_g, ranging from 0.3 to 14 m/s, and water superficial velocities j_l, ranging from 0.08 to 1.3 m/s.

MRI TECHNIQUE

The MRI has proven to be an effective method of visualizing blood flow by tracking the motion of protons. The proton density and the movement of the protons in the presence of a magnetic field gradient offer a noninvasive method to quantify the blood flow structure and flow velocity for an excited flow slice in any direction.[1]

The quantification of the flow velocity can be accomplished either by imaging spatial variations in the magnitude of the magnetization or by sensitizing the spatial orientation (the phase) of the magnetization to reflect the proton velocity.

Prior to tagging, the spins have equilibrium magnetization strength. Slice-selective saturation pulses can be used to label the magnetization of all spins within a selected slice. If this repetitive excitation is delivered to a tube carrying steady flow, a steady-state distribution of magnetization will be established. This steady state will consist of a train of volumes of magnetization strength induced by radio-frequency (rf) saturation excitation. An image of this distribution of magnetization will then show the displacement of fluid boli in the time interval *TR* between each excitation.

EXPERIMENT DESIGN

This preliminary study examines the single-phase laminar flow, two-phase stratified laminar flow, two-phase wavy laminar flow, and two-phase slug turbulent flow. For the two-phase flow cases, the volumetric flow rate of the air and of the liquid is measured prior to entering the mixing chamber. The air-water mixture travels concurrently through the 6-m tube and exits into a discharge tank that permits the air to separate from the liquid. The liquid is then recirculated through the test section.

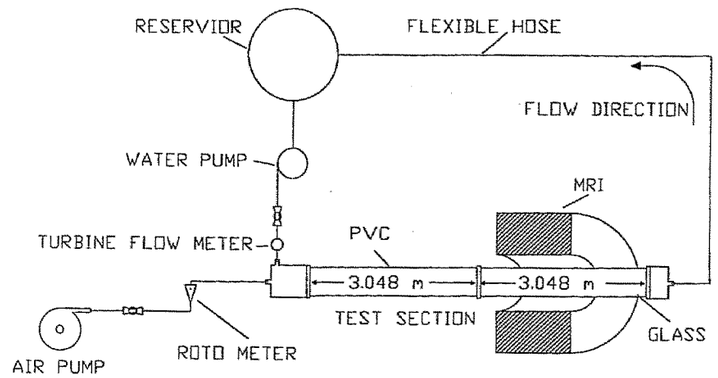

Fig. 1. General arrangement of the cocurrent air-water flow test.

The tube is located inside a 1.5-T MRI unit.[a] The scanner is a whole-body system and has a 55-cm-diam bore. The static magnetic field is generated by superconducting coils. The rf coils are used to transmit rf excitation into the material to be imaged. This excites a component of magnetization in the transverse plane that can be detected by an rf reception coil. To localize the signal in space, gradients of magnetic field are used to generate a variation of processional frequencies across the sample. The received signal reflects this distribution of frequencies, and a Fourier transform of the received signal provides an image of the spatial distribution of magnetization. The magnetic field gradients on this system are capable of a maximum gradient strength of 10 mT/m and can be ramped from zero to maximum strength in 1 ms.

A variety of MRI strategies were used to display different properties of the flow. The described bolus tagging method was used to provide a visualization of the distribution of velocities across the tube in longitudinal image planes. This sequence provided 6-mm-thick slices with an in-plane resolution of 1 × 1 mm. In addition, a spin echo sequence of a plane transverse to the flow direction was used to depict the isovelocity contours across the tube. These appear as alternate dark and bright bands of signal intensity.

By varying the liquid and air flow rates, a wide range of two-phase flow patterns could be produced in the test section. Using specialized scanning sequences, the MRI unit was capable of producing flow images of the *X-Y* plane, the *Y-Z* plane, and the *X-Z* plane.

The magnetic resonance images were recorded on the computer and processed using a software package called IMAGE.[b]

CONCLUSION

This initial feasibility study using advanced MRI scanning techniques for flow imaging has demonstrated that highly detailed data on two-phase flow structure and flow pattern transitions can be obtained. These data will provide new insights into flow structure and may permit the development of quantitative methods of characterizing two-phase flow patterns.

[a]Manufactured by Magnetom, Siemens, Erlangen, Germany.

1. D. SALONER, C. M. ANDERSON, "Flow Velocity Quantitation Using Inversion Tagging," *Magnetic Resonance in Medicine*, p. 16 (1989).

[b]From Wayne Rasband, National Institutes of Health, Bethesda, Maryland.